

Extended Press-Schechter theory and the density profiles of dark matter haloes

Nicos Hiotelis^{*} [†]

1st Experimental Lyceum of Athens, Ipitou 15, Plaka, 10557, Athens, Greece, E-mail: hiotelis@ipta.demokritos.gr

Accepted Received; in original form

ABSTRACT

An inside-out model for the formation of haloes in a hierarchical clustering scenario is studied. The method combines the picture of the spherical infall model and a modification of the extended Press-Schechter theory. The mass accretion rate of a halo is defined to be the rate of its mass increase due to minor mergers. The accreted mass is deposited at the outer shells without changing the density profile of the halo inside its current virial radius. We applied the method to a flat Λ CDM Universe. The resulting density profiles are compared to analytical models proposed in the literature, and a very good agreement is found. A trend is found of the inner density profile becoming steeper for larger halo mass, that also results from recent N-body simulations. Additionally, present-day concentrations as well as their time evolution are derived and it is shown that they reproduce the results of large cosmological N-body simulations.

Key words: cosmology: theory – dark matter – galaxies: haloes – structure – formation

1 INTRODUCTION

Numerical studies (Quinn, Salmon & Zurek (1986); Frenk et al. (1988); Dubinski & Galberg (1991); Crone, Evrard & Richstone (1994); Navarro, Frenk & White (1997), hereafter NFW; Cole & Lacey (1996); Huss, Jain & Steinmetz (1999); Fukushige & Makino (1997); Moore et al. (1998), hereafter MGQSL; Jing & Suto (2000), hereafter JS; Hernquist (1990), hereafter H90, Kravtsov et al. (1998), Klypin et al. (2001)) show that the density profiles of dark matter haloes are fitted by models of the form

$$\rho_f(r) = \frac{\rho_c}{(r/r_s)^\lambda [1 + (r/r_s)^\mu]^\nu} \quad (1)$$

More specifically NFW proposed a model with $\lambda = 1, \mu = 1, \nu = 2$, H90 proposed $\lambda = 1, \mu = 1, \nu = 3$, MGQSL $\lambda = 1.5, \mu = 1.5, \nu = 1$ while JS proposed $\lambda = 1.5, \mu = 1, \nu = 1.5$.

The logarithmic slope γ , of the density profile, defined by

$$\gamma(r) \equiv -\frac{d \ln \rho_f(r)}{d \ln r} = \lambda + \mu \nu \frac{(r/r_s)^\mu}{1 + (r/r_s)^\mu} \quad (2)$$

is, in all the above models, a decreasing function of radius. It is smaller than 2 near the centre of the system and larger near its virial radius.

An interesting quantity that characterizes the shape of the density profile is the concentration. This is defined by $c = R_{\text{vir}}/r_s$ where R_{vir} is the virial radius of the system. In a hierarchical clustering model, the concentration is a decreasing function of the mass of the system. Thus, smaller systems, that formed earlier, have higher concentrations than larger ones. This reflects the high density of the Universe at the epoch of their formation. The concentration of the resulting structures is studied in details by large N-body simulations. In particular, Bullock et al. (2001), BKPD hereafter, constructed a toy-model that describes accurately the time evolution of the concentration in a way consistent with the results of their large cosmological simulations.

Although numerical experiments are the most powerful method to study the formation of structures, the development of analytical or semi-numerical methods is very important as well since they help to improve our understanding about the physical processes during the formation. Density profiles of equilibrium cold dark matter haloes are studied by such methods (e.g. Syer & White (1998), Avila-Reese, Firmani & Hernández (1998), Raig, González-Casado & Salvador-Solé (1998), Henriksen & Widrow (1999), Nusser & Sheth (1999), Kull (1999), Lokas (2000), Hiotelis (2002)).

Modifications of the extended Press-Schechter theory (PS) (Press & Schechter (1974); Bower (1991); Bond et al. (1991), Lacey & Cole (1993)) based on the distinction between minor and major mergers (Manrique & Salvador-Solé (1996); Kitayama & Suto (1996); Salvador-Solé, Solanes & Manrique (1998), Cohn, Bagla & White (2001)) are also used

^{*} E-mail: hiotelis@ipta.demokritos.gr

[†] Present address: Roikou 17-19, Neos Kosmos, Athens, 11743 Greece

for studying the formation of structures. Recently, such a modified PS approximation was combined with a spherical infall model picture of formation by Manrique et al. (2003), MRSSS hereafter. Their results are in good agreement with those of N-body simulations.

In this paper we use the formalism of MRSSS, with justified modifications, and the same model parameters as in BKPD. We compare the characteristics of the resulting structures with those in N-body results. In Section 2, we discuss the modified PS theory and its application to the calculation of the density profile. In Section 3, the characteristics of the resulting dark matter haloes are presented. A discussion is given in Section 4.

2 EXTENDED AND MODIFIED PRESS-SCHECHTER THEORY

One of the major goals of the spherical infall model is the PS approximation. It states that the comoving density of haloes with mass in the range $M, M + dM$ at time t is given by the relation:

$$N(M, t)dM = \sqrt{\frac{2}{\pi}} \frac{\delta_c(t)}{\sigma^2(M)} \frac{\rho_{b0}}{M} e^{-\frac{\delta_c^2(t)}{2\sigma^2(M)}} \left| \frac{d\sigma(M)}{dM} \right| dM \quad (3)$$

where $\sigma(M)$ is the present-day rms mass fluctuation on comoving scale containing mass M and is related to the power spectrum P by the following relation

$$\sigma^2(M) = \frac{2}{\pi^2} \int \hat{W}^2(kR) P(k) k^2 dk \quad (4)$$

where \hat{W} is the Fourier transform of the window function used to smooth the overdensity field. The mass M and the radius R are related by the equation

$$M = \frac{4}{3} \pi \rho_{b0} R^3 = \frac{\Omega_{m0} H_0^2}{2G} R^3 \quad (5)$$

where ρ_{b0} is the present-day value of the density of the unperturbed Universe, Ω_{m0} is the present-day value of the density parameter (defined at any scale factor a by the relation $\Omega_m(a) = 8\pi G \rho_b(a)/(3H^2(a))$) and H_0 is the present-day value of Hubble's constant, H .

The only time dependent term of Eq. 3 is $\delta_c(t)$ that is the linear extrapolation up to the present epoch of the primordial density that collapses at t . It is calculated using the following arguments: In a model universe with cosmological constant Λ , the radius r of a sphere having initial overdensity Δ_i , evolves according to the equation

$$\frac{ds}{dt} = H_i g^{\frac{1}{2}}(s) \quad (6)$$

where $s \equiv r/r_i$ and r_i is the initial radius. H_i is the value of the Hubble's constant at the initial time t_i and g is given by the relation

$$g(s) = \Omega_{m,i}(1 + \Delta_i)(s^{-1} - 1) + \Omega_{\Lambda,i}(s^2 - 1) + 1 - \frac{2}{3}f_i\Delta_i \quad (7)$$

and $\Omega_{\Lambda,i}$ is the initial values of the quantity $\Omega_{\Lambda}(a) = \Lambda/(3H^2(a))$. Eq.7 is derived under the assumption that the initial velocity v_i of the shell is $v_i = H_i r_i - v_{pec,i}$ where the initial peculiar velocity, $v_{pec,i}$, is given according to the

linear theory by the relation $v_{pec,i} = \frac{1}{3}H_i r_i f_i \Delta_i$ (Peebles (1980)). A very good approximation of the factor f_i is $f_i = \Omega_{m,i}^{0.6} + \frac{1}{70}[1 - \Omega_{m,i}(1 + \Omega_{m,i})]$ (Lahav et al. (1991)). The radius of the maximum expansion is $r_{ta} = s_{ta}r_i$, where s_{ta} is the root of the equation $g(s) = 0$ that corresponds to zero velocity ($ds/dt = 0$). The sphere reaches its turnaround radius at time

$$t_{ta} = \frac{1}{H_i} \int_0^{s_{ta}} g^{-\frac{1}{2}}(s) ds \quad (8)$$

and then collapses at time $t_c = 2t_{ta}$.

The scale factor a of the Universe obeys the equation:

$$\frac{da}{dt} = H_0 X^{\frac{1}{2}}(a) \quad (9)$$

where

$$X(a) = 1 + \Omega_{m,0}(a^{-1} - 1) + \Omega_{\Lambda,0}(a^2 - 1) \quad (10)$$

and the subscript 0 denotes the present-day values of the parameters. However, the time and the scale factor a are related by the equation

$$t = \frac{1}{H_0} \int_0^a X^{-\frac{1}{2}}(u) du \quad (11)$$

Setting $t = t_c$ in the above equation and solving for a one finds the scale factor a_c at the epoch of collapse. If we call $\delta_{i,c}(t)$ the initial overdensity required for the spherical region to collapse at that time t and take into account the linear theory for the evolution of the matter density contrast $\delta = \delta\rho/\rho$, we have

$$\delta \propto \frac{1}{H_0^2} \frac{X^{1/2}(a)}{a} \int_0^a X^{-3/2}(u) du = D(a), \quad (12)$$

(Peebles 1980), then $\delta_c(t)$ is given

$$\delta_c(t) = \delta_{i,c}(t) \frac{D(t_0)}{D(t_i)}, \quad (13)$$

where t_0 denotes the present epoch.

Usually δ_c is written in the form

$$\delta_c(t) = \delta_{i,c}(t) \frac{D(t)}{D(t_i)} \frac{D(t_0)}{D(t)} = \delta_{crit}(t) \frac{D(t_0)}{D(t)} \quad (14)$$

where $\delta_{crit}(t)$ is the linear extrapolation of the initial overdensity up to the time t of its collapse. In an Einstein-de Sitter universe ($\Omega_m = 1, \Omega_{\Lambda} = 0$) this value is independent on the time of collapse and is $\delta_{crit} \approx 1.686$. In other cosmologies it has a weak dependence on the time of collapse (e.g. Eke, Cole & Frenk (1996)). In a flat universe it can be approximated by the formula $\delta_{crit}(t) \approx 1.686\Omega_{m,0}^{0.0055}(t)$.

The PS mass function agrees relatively well with the results of N-body simulations (e.g. Efstathiou, Frenk & White (1985), Efstathiou & Rees (1988); White, Efstathiou & Frenk (1993), Lacey & Cole (1994); Gelb & Bertschinger (1994); Bond & Myers (1996)) while it deviates in detail at both the high and low masses. Recent improvements (Sheth & Tormen (1999); Sheth, Mo & Tormen (2001), see also Jenkins et al.(2001)) allow a better approximation involving some more parameters. The application of the above approximation to the model studied in this paper is a subject of future research.

Lacey & Cole (1993) extended the PS theory using the idea of a Brownian random walk, and were able to calculate analytically tractable expressions for the mass function,

merger rates, and other properties. They show that the instantaneous transition rate at t from haloes with mass M to haloes with mass between $M', M' + dM'$ is given by

$$r(M \rightarrow M', t) dM' = \left(\frac{2}{\pi}\right)^{1/2} \frac{d\delta_c(t)}{dt} \frac{1}{\sigma^2(M')} \frac{d\sigma(M')}{dM'} \left[1 - \frac{\sigma^2(M')}{\sigma^2(M)}\right]^{-3/2} \times \exp\left[-\frac{\delta_c^2(t)}{2} \left(\frac{1}{\sigma^2(M')} - \frac{1}{\sigma^2(M)}\right)\right] dM' \quad (15)$$

This provides the fraction of the total number of haloes with mass M at t , which give rise per unit time to haloes with mass in the range $M', M' + dM'$ through instantaneous mergers of any amplitude.

An interesting modification of the extended PS theory is the distinction between minor and major mergers (Manrique & Salvador-Solé (1996); Kitayama & Suto (1996); Salvador-Solé et al. (1998); Percival, Miller & Peacock (2000), Cohn et al. (2001)).

Mergers that produce a fractional increase below a given threshold Δ_m are regarded as minor. This kind of mergers corresponds to an accretion. Consequently, the rate at which haloes increase their mass due to minor mergers is the instantaneous mass accretion rate and is given by the relation

$$r_m^a(M, t) = \int_M^{M(1+\Delta_m)} (M' - M) r(M \rightarrow M', t) dM' \quad (16)$$

Thus the rate of the increase of halo's mass due to the accretion is

$$\frac{dM(t)}{dt} = r_m^a[M(t), t] \quad (17)$$

Before proceeding further with the model, it is useful to discuss briefly the cosmological considerations about the virial radius of a spherical system. Let $\Delta_{\text{vir}}(a)$ be the ratio of the overdensity of a sphere, that has collapsed and virialized at scale factor a , to the background density. This can be expressed by the form:

$$\Delta_{\text{vir}}(a) = \frac{\rho(a)}{\rho_b(a)} = \frac{1}{s_{ta}^3 c_f^3} \left(\frac{a}{a_i}\right)^3 (1 + \Delta_i) \quad (18)$$

where c_f is the collapse factor of the sphere defined as the ratio of its final radius to its turnaround radius. Lahav et al. (1991) applied the virial theorem to the virialized final sphere assuming a flat overdensity and found the collapse factor to be $c_f \approx (1 - n/2)/(2 - n/2)$ where $n = (\Delta r_{ta}^3)/(3GM)$. For an Einstein-de Sitter Universe $\Delta_{\text{vir}}(a) \approx 18\pi^2$ at any time. For flat models with cosmological constant, significantly good analytical approximations of Δ_{vir} exist. Bryan & Norman (1998) proposed for Δ_{vir} the following approximation

$$\Delta_{\text{vir}}(a) \approx (18\pi^2 - 82x - 39x^2)/\Omega_m(a) \quad (19)$$

where $x \equiv 1 - \Omega_m(a)$.

MRSSS considered the following picture of the formation of a halo: At time t_i an halo of virial mass M_i and virial radius R_i is formed and at later times it accretes mass according to the Eq.(17). Assuming that the accreted mass is deposited in an outer spherical shell without changing the density profile inside its current radius, then

$$M_{\text{vir}}(t) - M_i = \int_{R_i}^{R_{\text{vir}}(t)} 4\pi r^2 \rho(r) dr \quad (20)$$

The current radius R_{vir} contains a mass with mean density $\Delta_{\text{vir}}(a)$ times the mean density of the Universe $\rho_b(t)$. Therefore,

$$R_{\text{vir}}(t) = \left[\frac{3M_{\text{vir}}(t)}{4\pi\Delta_{\text{vir}}(t)\rho_b(t)} \right]^{1/3} \quad (21)$$

Differentiating with respect to t

$$\rho(t) = \Delta_{\text{vir}}(t)\rho_b(t) \left[1 - \frac{M_{\text{vir}}(t)}{r_m^a[M_{\text{vir}}(t), t]} \frac{d[\ln[\rho_b(t)\Delta_{\text{vir}}(t)]]}{dt} \right]^{-1} \quad (22)$$

Since one of the goals of this paper is the comparison of our results with the results of the N-body simulations of BKPD, we have used for $\Delta_{\text{vir}}(t)$ the same approximation as BKPD did -that is Eq.19- and not the constant value of 200 that MRSSS used. It is convenient to express Eq.22 in terms of the scale factor a instead of the time t . Thus, Eq.22 becomes:

$$\rho(a) = \frac{3H^2(a)\Omega_m(a)}{8\pi G} \Delta_{\text{vir}}(a) \times \left[1 + \frac{M_{\text{vir}}(a)}{r_m^{\text{acc}}[M_{\text{vir}}(a), a]} \left(\frac{3}{a} - \frac{d \ln[\Delta_{\text{vir}}(a)]}{da} \right) \right]^{-1} \quad (23)$$

where we used $\rho_b(a)a^3 = \text{const.}$ and

$$r_m^{\text{acc}}[M_{\text{vir}}(a), a] \equiv \frac{dM_{\text{vir}}}{da} = H_0^{-1} X^{-1/2}(a) r_m^a[M_{\text{vir}}(t), t]. \quad (24)$$

Integrating Eq.17 and using Eqs. 21 and 23, we obtain the growth of virial mass and virial radius and, in a parametric form, the density profile of haloes.

3 DENSITY PROFILES OF DARK MATTER HALOES

The results described in this section are derived for a flat universe with $\Omega_{m,0} = 0.3$ and $\Omega_{\Lambda,0} = 0.7$. We used two forms of power spectrum. The first one -named spect1- is the one proposed by Efstathiou, Bond & White (1992). It is based on the results of the COBE DMR experiment and is given by the relation:

$$P_{\text{spect1}}(k) = \frac{Bk}{[1 + [ak + (bk)^{3/2} + (ck)^2]^{\nu}]^{2/\nu}} \quad (25)$$

where $a = (6.4/\Gamma)h^{-1}\text{Mpc}$, $b = (3.0/\Gamma)h^{-1}\text{Mpc}$, $c = (1.7/\Gamma)h^{-1}\text{Mpc}$ and $\nu = 1.13$. Low-density Cold Dark Matter (CDM) models in a spatially flat Universe (i.e. $\Lambda > 0$) are described for $\Gamma = \Omega_{m,0}h$.

The second spectrum -named spect2- is the one proposed by Smith et al. (1998) and is given by:

$$P_{\text{spect2}}(k) = \frac{Ak^n}{[1 + a_1 k^{1/2} + a_2 k + a_3 k^{3/2} + a_4 k^2]^b} \quad (26)$$

The values for the parameters are: $n = 1$, $a_1 = -1.5598$, $a_2 = 47.986$, $a_3 = 117.77$, $a_4 = 321.92$ and $b = 1.8606$.

We used the top-hat window function that has a Fourier transform given by:

$$\hat{W}(kR) = \frac{3(\sin(kR) - kR \cos(kR))}{(kR)^3} \quad (27)$$

The constants of proportionality A and B are found using the procedure of normalization for $\sigma_8 \equiv \sigma(R = 8h^{-1}\text{Mpc}) = 1$. In Fig.1, the resulting rms fluctuations for both spectra

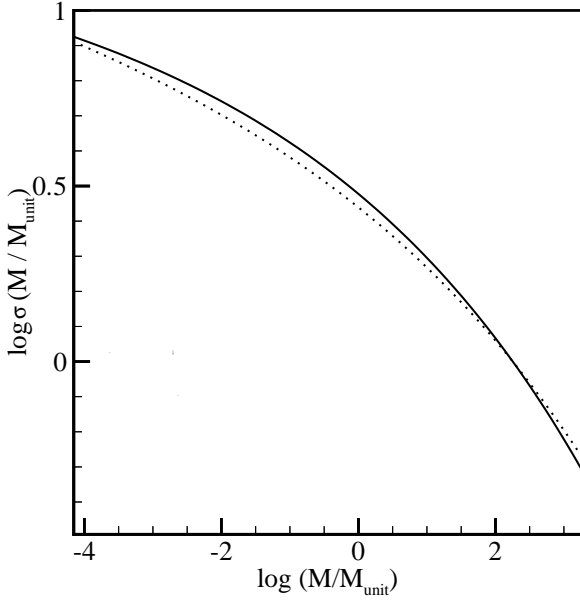


Figure 1. rms mass fluctuation as a function of mass. Solid line: for spect1, dotted line: for spect2

are shown. It must be noted that we use a system of units with $M_{\text{unit}} = 10^{12} h^{-1} M_{\odot}$, $R_{\text{unit}} = h^{-1} \text{Mpc}$ and $t_{\text{unit}} = 1.515 \times 10^7 h^{-1} \text{years}$. In this system of units $H_0/H_{\text{unit}} = 1.5276$.

3.1 Present day structures

In the approximation used in this paper, for given models of the Universe and power spectrum there is only one free parameter, that is the value of the threshold Δ_m (see Eq.16). We found that the resulting density profiles are sensitive to the value of Δ_m . As an example, the density profiles of two systems with the same present-day mass $10^{12} h^{-1} M_{\odot}$ and different values of Δ_m are plotted in Fig.2. Both density profiles are derived from spect2. The solid line -shown in Fig.2- corresponds to the system derived for $\Delta_m = 0.21$ while the dotted line to the system for $\Delta_m = 0.5$. The density profile for smaller Δ_m is steeper at both the inner and the outer regions. Additionally, for different Δ_m the concentrations of the haloes are different too (a detailed description of the way the concentration is calculated is given below). The system that results for $\Delta_m = 0.21$ has $c_{\text{vir}} = 15.2$, while the one for $\Delta_m = 0.5$ has $c_{\text{vir}} = 8.7$. In order to calculate the density profiles (that will be presented below), we used as a basic criterion the concentrations of the present-day structures. In fact, we have chosen the values of $\Delta_m = 0.23$ and $\Delta_m = 0.21$ for spect1 and spect2 respectively, because the concentrations resulting from these values are close to the results of the toy-model of BKPD. This model is constructed by BKPD to reproduce the results of their N-body simulations and it is able to give the concentration c_{vir} of a virial mass M_{vir} at any scale factor a . First, the scale factor a_c at the epoch of collapse is calculated, solving the following equation

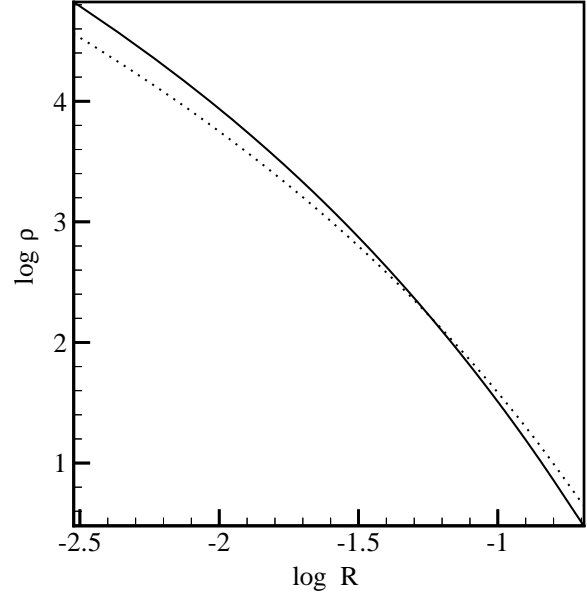


Figure 2. For spect2: Density profiles for two haloes having the same mass $10^{12} h^{-1} M_{\odot}$. Solid line: $\Delta_m = 0.21$. Dotted line: $\Delta_m = 0.5$

$$\sigma[M_*(a_c)] = \sigma[FM_{\text{vir}}(a)] \quad (28)$$

where $F = 0.01$ and M_* is the typical collapsing mass. Then, the concentration is calculated using the formula

$$c_{\text{vir,BKPD}}[M_{\text{vir}}(a), a] = K \frac{a}{a_c} \quad (29)$$

where $K = 4$. We recall that the typical collapsing mass at scale factor a satisfies $\sigma[M_*(a)] = 1.686 D(1)/D(a)$.

It is obvious that the above defined concentration depends only on the cosmology and the power spectrum used. Thus, for given cosmology and halo mass, the concentration $c_{\text{vir,BKPD}}$ is known *a priori* without taking into consideration any particular form of halo growth. We applied this toy-model to find $c_{\text{vir,BKPD}}$ for the present-day structures.

Another way to calculate the concentration is by using $c_{\text{vir}} = R_{\text{vir}}/r_2$ where r_2 is the radius where the logarithmic slope of the density profile equals 2. This radius is found by the following procedure: First, the resulting density profiles are fitted by the general formula of Eq.1. This is done by minimizing the sum

$$S = \sum [\rho(r) - \rho_f(r)]^2. \quad (30)$$

where ρ_c , r_s , λ , μ and ν are fitting parameters. The minimization is performed using the unconstrained subroutine ZXNWD of IMSL mathematical library. Then, r_2 is found by applying the following formula for $n = 2$

$$r_n = \left[\frac{n - \lambda}{\lambda + \mu\nu - n} \right]^{1/\mu} r_s \quad (31)$$

This formula gives the radius r_n at which the logarithmic slope equals to n . According to the model presented in this paper, haloes grow inside-out. Thus, the value of c_{vir} represents the way of halo growth. In Fig. 3, the concentration is

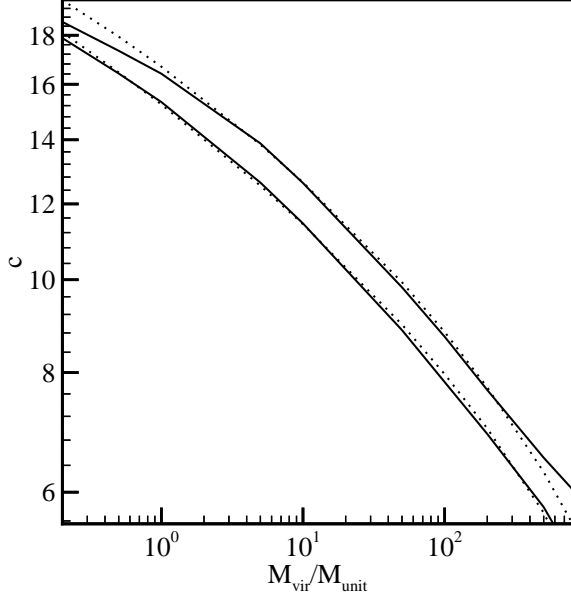


Figure 3. Concentration as a function of present-day virial mass. From the top, the first pair of curves are for spect1 and the second for spect2. Solid curves: our results. Dotted curves: BKPD toy-model results.

plotted as a function of the present-day virial mass. From the top of the figure, the first pair of curves (solid and dotted) correspond to spect1 and the second pair to spect2. Solid curves show our results while dotted curves depict the results of the toy-model of BKPD. A very good agreement between the values of the concentration is shown. In particular, concentrations resulting from spect2 are in agreement with those obtained for the model of BKPD for the whole range of mass presented. On the other hand, small differences appear for very small and very large masses in the case of spect1.

In Fig. 4 we present the density profiles of the resulting structures with present-day masses in the range of $0.2 \times 10^{11} h^{-1} M_{\odot}$ to $8 \times 10^{14} h^{-1} M_{\odot}$. The left-hand side figures (a1, b1, c1, d1, e1) have been produced using spect1, while the right-hand ones using spect2. Figures (a1) and (a2) correspond to mass $0.2 \times 10^{11} h^{-1} M_{\odot}$, (b1) and (b2) have mass $10^{12} h^{-1} M_{\odot}$, (c1) and (c2) to mass $10^{13} h^{-1} M_{\odot}$, (d1) and (d2) to mass $10^{14} h^{-1} M_{\odot}$ and (e1) and (e2) correspond to mass $8 \times 10^{14} h^{-1} M_{\odot}$. Solid lines represent the resulting density profiles while dotted lines are the fits using the general formula of Eq.1. It is shown that the fits using the general formula of Eq.1 are exact. We also fit every halo density profile using the analytical models that have been proposed in the literature (H90, NFW, MGQSL, JS) and are described in Section 1. The best fit of these models to our resulting profiles is shown in Fig. 4 (circles). This best fit is found by the minimizing procedure described above, for λ , μ and ν constants and equal to the proposed values, while ρ_c and r_s are the only fitting parameters. Best fit for the resulting density profile in (a1) is the H90 model, in (a2) and (b2) the NFW model, in (b1), (c1) and (c2) the MGQSL model

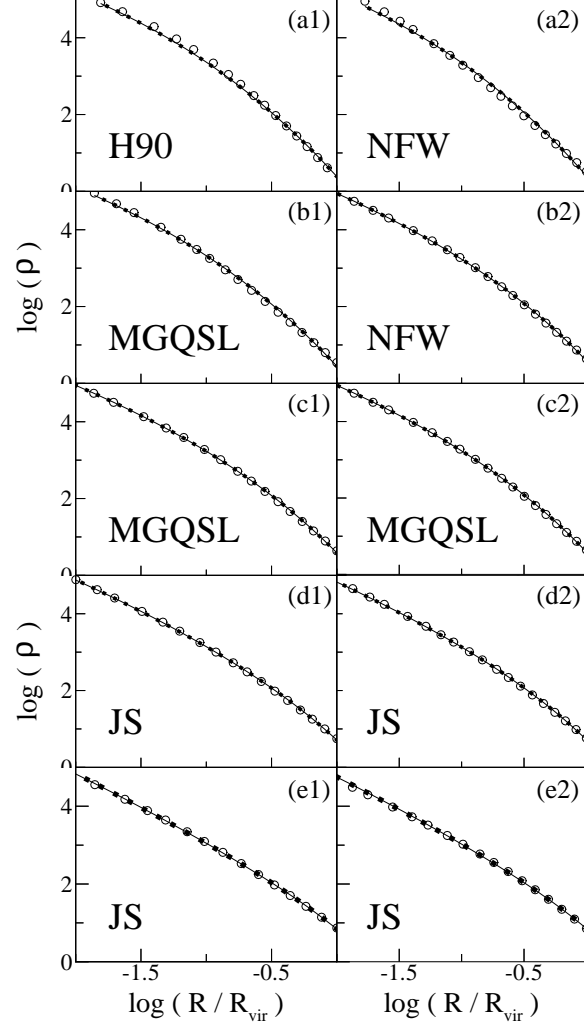


Figure 4. Density profiles as a function of radius. Solid curves: resulting density profiles. Dotted curves: fits of the resulting density profiles using the formula of Eq.1. Circles: best fit to our results using models proposed in the literature (H90, NFW, MGQSL, JS). Left-hand side: spect1. Right-hand side: spect2

and in (d1), (d2), (e1) and (e2) the JS model. Additionally, haloes of different mass are fitted well by different analytical models. This is due to the different inner and outer slopes of the density profiles. Inner slope, (defined as that at radial distance $r = 10^{-2} R_{\text{vir}}$), is an increasing function of the virial mass of the halo. For example, in the case of spect2 the inner slope varies from 1.43 for $M = 10^{12} h^{-1} M_{\odot}$ to 1.65 for $M = 8 \times 10^{14} h^{-1} M_{\odot}$. Additionally, outer slope -at $r = R_{\text{vir}}$ - is a decreasing function of the virial mass and it varies from 3.67 to 2.64 for the above range of masses.

Although density profiles resulting in simulations seem to be similar, systematic trends that relate them with the power spectrum have been reported. For example, Subramanian, Cen & Ostriker (2000) found in the results of their N-body simulations the following: for power spectra of the form $P(k) \propto k^n$ the density profiles have steeper cores for larger n . Therefore, a dependence of the density profile on the power spectrum is expected. This dependence is shown in our results comparing the profiles of haloes with the same

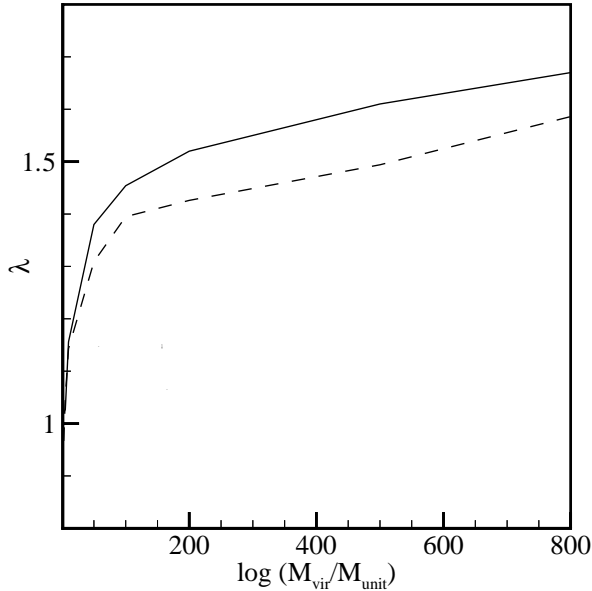


Figure 5. Exponent λ as a function of present-day virial mass for both power spectra. It is shown that λ is an increasing function of the virial mass. Solid curve: spect1. Dashed curve: spect2

present day mass. It should be noted that the method studied in this manuscript is applicable for the era of slow accretion when the infalling matter is in the form of small haloes that have mass less than Δm times the mass of the parent halo. This kind of accretion occurs at the late stages of formation and thus determines the profile of the outer regions of the halo under study. However, the values of the inner slopes may be questionable. Real haloes have followed different mass growth histories and thus their properties show a significant scatter about a mean value. Unfortunately, the method studied in this manuscript results one profile for a halo of given mass. Thus, its purpose is just to approximate the mean density profile of a large number of mass growth histories. Since the mass growth history resulting from the method is in good agreement with the mean growth history resulting from N-body simulation -as it will be shown below- then the values of the inner slopes could be close to the ones of N-body simulations. A Monte Carlo analytic approach based on the construction of a large number of mass accretion histories is under study. This study could answer to some of the above problems.

In Fig. 5 the exponent λ is plotted, that gives the asymptotic slope at $R \rightarrow 0$, derived by the general fit as a function of present-day virial mass for both power spectra. It is shown that the exponent λ is an increasing function of virial mass. This trend of the inner density profile is also found in the results of recent N-body simulations (Ricotti (2002)).

3.2 Time evolution

In Fig. 6 we plot mass growth curves. The curves show $M_{\text{vir}}(a)$ as a function of a in a logarithmic slope. The solid

lines show our resulting structures and the dotted lines show the mass growth curves of the model proposed by Wechsler et al. (2002). The curves of the left panel correspond to spect1 while those of the right panel to spect2. From the top to the bottom, the curves correspond to masses $2 \times 10^{11} h^{-1} M_{\odot}$, $10^{12} h^{-1} M_{\odot}$, $10^{13} h^{-1} M_{\odot}$, $10^{14} h^{-1} M_{\odot}$ and $8 \times 10^{14} h^{-1} M_{\odot}$ respectively. It is obvious that massive haloes show substantial increase of their mass up to late times while the growth curves of less massive haloes tend to flatten out earlier. This behaviour of mass growth curves characterizes the hierarchical clustering scenario where small haloes are formed earlier than more massive ones. Additionally, it helps to define the term "formation time" by a measurable way. Wechsler et al. (2002) define as formation scale factor \tilde{a}_c the scale factor when the logarithmic slope of mass growth, $(d \ln M(a)/d \ln a)$, falls below some specified value, S . They use the value $S = 2$. It should be noted that this definition of formation scale factor differs from a_c , defined by BKPD, since a_c is the value of the scale factor at the epoch the typical collapsing mass is F times the virial mass of the halo. We found that the values of \tilde{a}_c and a_c for $F = 0.01$ and $S = 2$ are different. This is also noticed in Wechsler et al. (2002) since they state that \tilde{a}_c and a_c have similar values for $S = 2$ but for $F = 0.015$. However, the use of the value $F = 0.015$ in the toy-model of BKPD changes the resulting concentrations and so our basic criterion for the choice of the threshold Δ_m is not satisfied. Therefore, it is preferable to choose a different value of S for the definition of \tilde{a}_c , that of $S = 1.5$. In Fig. 6, the dotted lines show the mass growth curves of the model proposed by Wechsler et al. (2002). In this model the mass growth is calculated using the relation:

$$M_{\text{vir}}(a) = M_{\text{vir},0} \exp[-\tilde{a}_c S (1/a - 1)] \quad (32)$$

where $M_{\text{vir},0}$ is the present-day virial mass and the formation scale factor \tilde{a}_c is defined by the condition $d \ln M(a)/d \ln a = S$ with $S = 1.5$. In Fig. 6, a very satisfactory agreement is shown, particularly for the less massive haloes.

We have to note that our model haloes grow inside-out. Therefore, in early enough times -when the slope of the density is smaller than 2 all the way from the centre up to the current radius- it is meaningless to define c_{vir} . Once the building of the halo has proceeded beyond the point with slope 2, the evolution of c_{vir} is due to the growth of the virial radius and is given by

$$c_{\text{vir}}[M(a), a] = c_{\text{vir}}(M_0) \frac{R_{\text{vir}}[M(a)]}{R_{\text{vir}}(M_0)}, \quad (33)$$

where $c_{\text{vir}}(M_0)$ denotes the present-day concentration and $R_{\text{vir}}[M(a)]$ and $R_{\text{vir}}(M_0)$ are the values of the virial radius at scale factor a and at the present-day respectively. In Fig. 7 the time evolution of concentrations is plotted. Solid lines describe c_{vir} while dotted lines are $c_{\text{vir},\text{BKPD}}$. More massive haloes have lower concentrations that evolve slower, while the concentrations of less massive haloes are higher and evolve more rapidly.

4 CONCLUSIONS

Since the formation of structures in a hierarchical clustering scenario is a complicated process, any attempt for the con-

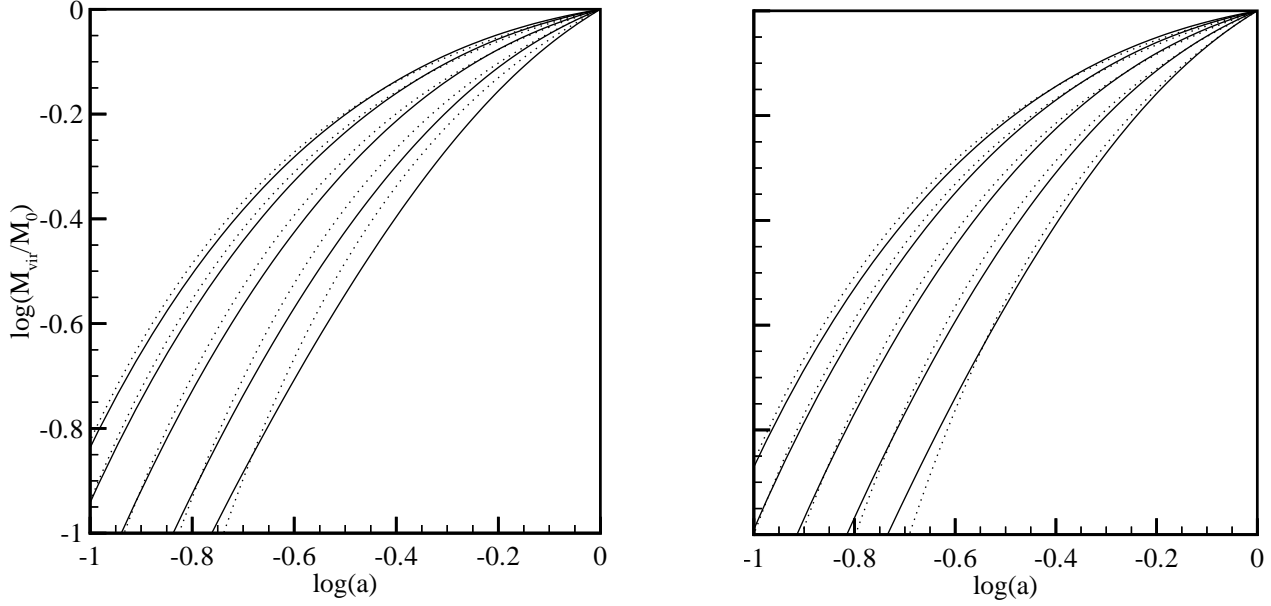


Figure 6. Mass growth curves as a function of scale factor a . Left panel, right panel: spect1, spect2 respectively. From top to the bottom the curves correspond to masses $0.2 \times 10^{11} h^{-1} M_{\odot}$, $10^{12} h^{-1} M_{\odot}$, $10^{13} h^{-1} M_{\odot}$, $10^{14} h^{-1} M_{\odot}$ and $8 \times 10^{14} h^{-1} M_{\odot}$ respectively.

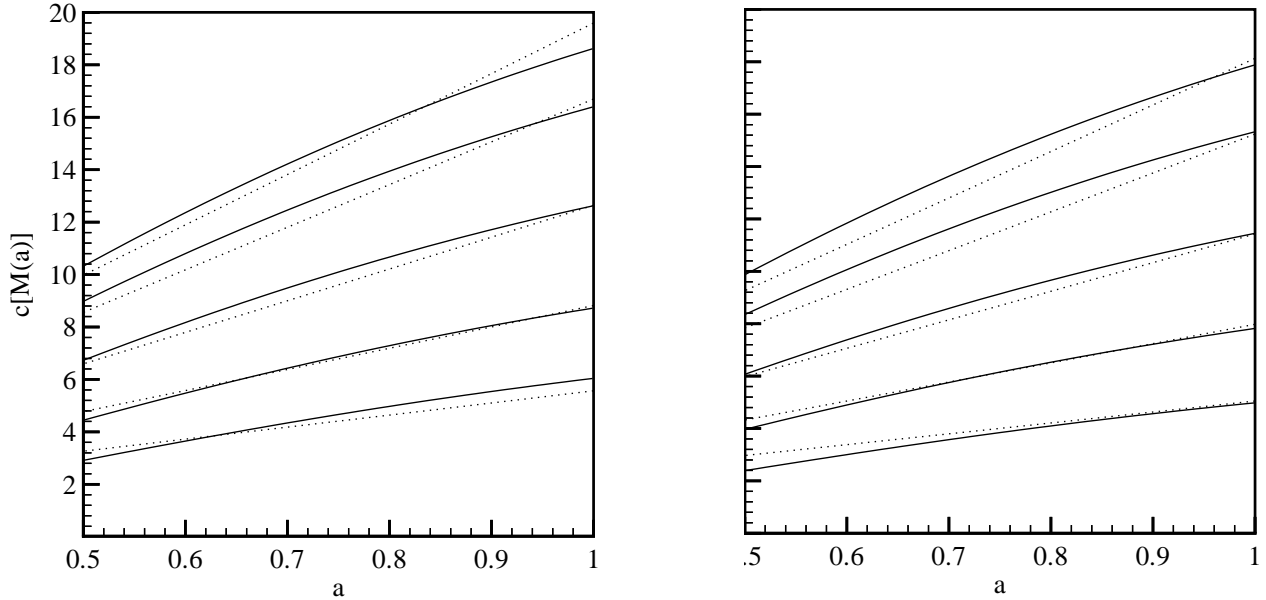


Figure 7. Concentration as a function of the scale factor a . Left panel: spect1. Right panel: spect2. Solid lines: our results. Dotted lines: the results of toy-model of BKPD. From top to the bottom the lines correspond to masses $0.2 \times 10^{11} h^{-1} M_{\odot}$, $10^{12} h^{-1} M_{\odot}$, $10^{13} h^{-1} M_{\odot}$, $10^{14} h^{-1} M_{\odot}$ and $8 \times 10^{14} h^{-1} M_{\odot}$ respectively.

struction of analytical models requires a number of crucial assumptions.

The model studied in this paper was proposed by MRSSS and assumes that

(i) The rate of mass accretion is defined by the rate of minor mergers

(ii) Haloes grow inside-out. The accreted mass is deposited at the outer shells without changing the density profile of the halo inside its current virial radius

The first assumption indicates that structures presented in this paper formed by a gentle accretion of mass. The physical process implied by the second assumption is that the infalling matter does not penetrate the current virial radius. This process requires an amount of non-radial motion. This amount has to be large enough so that the pericenter of the accreted mass is larger than the current virial radius. It should be noted that a density profile that results from a radial collapse has inner slope steeper than 2. It is the presence of non-radial motion during the collapse that leads to inner slopes shallower than 2. (e.g. Nusser (2001), Hiotelis (2002), Subramanian, Cen & Ostriker (2000)). Non-radial motions are always present in the structures formed in N-body simulations.

Despite the above assumptions, the results of the model studied in this paper are in good agreement with the results of N-body simulations. The summary of these results is as follows:

(i) Density profiles of haloes are close to the analytical models proposed in the literature as good fits to the results of N-body simulations. A trend of the inner slope of the density profile as an increasing function of the mass of the halo is also found, in agreement with recent results of N-body simulations.

(ii) Concentration is a decreasing function of virial mass. Its values are in agreement with the results of numerical methods.

(iii) Massive haloes increase their mass substantially up to late times. Growth curves of less massive haloes tend to flatten out earlier. The concentrations of less massive haloes evolve more rapidly while those of more massive haloes evolve slowly.

Taking into account the number of assumptions and approximations used to build the model presented in this paper, we can conclude that the agreement with the results of N-body simulations is very good. Consequently, this model provides a very promising method to deal with the process of structure formation. Further improvements to this model could help to understand better the physical picture during this process.

5 ACKNOWLEDGEMENTS

I would like to thank the *Empirikion Foundation* for its financial support.

REFERENCES

- Avila-Reese V., Firmani C., Hernández X., 1998, *ApJ*, 505, 37
- Bond J.R., Cole S., Efstathiou G., Kaiser N., 1991, *ApJ*, 379, 440
- Bond J.R., Myers S., 1996, *ApJS*, 103, 41
- Bower R.J., 1991, *MNRAS*, 248, 332
- Bryan G., Norman M., 1998, *ApJ*, 495, 80.
- Bullock J.S., Kolatt A., Primack J.R., Dekel A., 2001, *MNRAS*, 321, 559 (BKPD)
- Cohn J.D., Bagla J.S., White M., 2001 *MNRAS*, 325, 1053
- Cole S., Lacey C., 1996, *MNRAS*, 281, 716
- Crone M.M., Evrard A.E., Richstone D.O., 1994, *ApJ*, 434, 402
- Dubinski J., Calberg R., 1991, *ApJ*, 378, 496.
- Efstathiou G., Frenk C.S., White S.D.M., 1985, *ApJ*, 292, 371
- Efstathiou G., Rees M., 1988, *MNRAS*, 230, 5
- Efstathiou G., Bond J.R., White S.D.M., 1992, *MNRAS*, 258, 1
- Eke V.R., Cole S., Frenk C.S., 1996, *MNRAS*, 282, 263
- Frenk C.S., White S.D.M., Davis M., Efstathiou G., 1988, *ApJ*, 327, 507
- Fukushige T., Makino J., 1997, *ApJ*, 477, L9
- Gelb J., Bertschinger E., 1994, *ApJ*, 436, 467
- Henriksen R.N., Widrow L.M., 1999, *MNRAS*, 302, 321
- Hernquist L., 1990, *ApJ*, 356, 359
- Hiotelis N., 2002, *A&A*, 382, 84
- Huss A., Jain B., Steinmetz M., 1999, *MNRAS*, 308, 1011
- Jenkins A., Frenk C.S., White S.D.M., Colberg J.M., Cole S., Evrard A.E., Couchman H.M.P., Yoshida N., 2001, *MNRAS*, 321, 372
- Jing Y.P., Suto Y., 2000, *ApJ*, 529, L69 (JS)
- Kitayama T., Suto Y., 1996, *MNRAS*, 280, 638
- Kravtsov A.V., Klypin A.A., Bullock J.S., Primack J.R., 1998, *ApJ*, 502, 48
- Klypin A.A., Kravtsov A.V., Bullock J.S., Primack J.R., 2001, *ApJ*, 554, 903
- Kull A., 1999, *ApJ*, 516, L5
- Lacey C., Cole S., 1993, *MNRAS*, 262, 627
- Lacey C., Cole S., 1994, *MNRAS*, 271, 676
- Lahav O., Lilje P.B., Primack J.R., Rees M.J., 1991, *MNRAS*, 251, 128
- Lokas E.L., 2000, *MNRAS*, 311, 423
- Manrique A., Salvador-Solé E., 1996, *ApJ*, 467, 504
- Manrique A., Raig A., Salvador-Solé E., Sanchis T., Solanes J.M., 2003, preprint (astro-ph/0304378) (MRSSS)
- Moore B., Governato F., Quinn T., Stadel J. Lake G., 1998, *ApJ*, 499, L5 (MGQSL)
- Navarro J.F., Frenk C.S. White S.D.M., 1997, *ApJ*, 490, 493 (NFW)
- Nusser A., Sheth R., 1999, *MNRAS*, 303, 685
- Nusser A., 2001, *MNRAS*, 325, 1397
- Peebles P.J.E., 1980, *The Large-Scale Structure of the Universe*, Princeton Univ. Press, Princeton, NJ
- Percival W.J., Miller L., Peacock J.A., 2000, *MNRAS*, 318, 273
- Press W.H., Schechter P., 1974, *ApJ*, 187, 425.
- Quinn P.J., Salmon J.K., Zurek W.H., 1986, *Nature*, 322, 329
- Raig A., González-Casado G., Salvador-Solé, 1998, *ApJ*, 508, L129
- Ricotti M., 2002, preprint (astro-ph/0212146)
- Salvador-Solé E., Solanes J.M., Manrique A., 1998, *ApJ*, 499, 542
- Sheth R.K., Tormen G., 1999, *MNRAS*, 308, 119
- Sheth R.K., Mo H.J., Tormen G., 2001, *MNRAS*, 323, 1
- Smith C.C., Klypin A., Gross M.A. K., Primack J.R., Holtzman J., 1998, *MNRAS*, 297, 910
- Subramanian K., Cen R.Y., Ostriker J.P., 2000, *ApJ*, 538, 528
- Syer D., White S.D.M., 1988, *MNRAS*, 293, 337
- Wechsler R.H., Bullock J.S., Primack J.R., Kravtsov A.V., Dekel A., 2002, *ApJ*, 568, 52

White S.D.M., Efstathiou G., Frenk C., 1993, MNRAS,
262, 1023

This paper has been typeset from a T_EX/ L^AT_EX file prepared
by the author.